Original Article

Multiple basic amino acids in the cleavage site of H7N9 hemagglutinin contribute to high virulence in mice

Wenjun Song[1,2#], Xiaofeng Huang[2#†], Wenda Guan[1#], Pin Chen[2], Pui Wang[2], Min Zheng[2‡], Zhengtu Li[1], Yutao Wang[1], Zifeng Yang[1], Honglin Chen[2], Xinhua Wang[1]

[1]State Key Laboratory of Respiratory Disease, Institute of Integration of Traditional and Western Medicine, First Affiliated Hospital of Guangzhou Medical University, Guangzhou, China; [2]State Key Laboratory for Emerging Infectious Diseases, Department of Microbiology, and the Research Centre of Infection and Immunology, The University of Hong Kong, Hong Kong SAR, China

Contributions: (I) Conception and design: W Song, X Huang, H Chen; (II) Administrative support: H Chen, X Wang; (III) Provision of study materials or patients: W Guan, Z Li, Y Wang, Z Yang; (IV) Collection and assembly of data: W Guan, P Chen, P Wang, M Zheng; (V) Data analysis and interpretation: W Song, X Huang; (VI) Manuscript writing: All authors; (VII) Final approval of manuscript: All authors.

[#]These authors contributed equally to this work.

Correspondence to: Honglin Chen. State Key Laboratory for Emerging Infectious Diseases, Department of Microbiology, and the Research Centre of Infection and Immunology, The University of Hong Kong, 21 Sassoon Road, Hong Kong SAR, China. Email: hlchen@hku.hk; Xinhua Wang. State Key Laboratory of Respiratory Disease, Institute of Integration of Traditional and Western Medicine, First Affiliated Hospital of Guangzhou Medical University, 195 Dong Feng Road (W), Guangzhou 510180, China. Email: xinhuaw@gzhmu.edu.cn.

Background: Avian influenza A (H7N9) virus has caused more than 1,500 cases of human infection since its emergence in early 2013. Displaying little or no pathogenicity in poultry, but a 40% case-fatality rate in humans, five waves of H7N9 human infections occurred in China during 2013–2017, caused solely by a low pathogenicity strain. However, avian isolates possessing a polybasic connecting peptide in the hemagglutinin (HA) protein were detected in mid-2016, indicating that a highly pathogenic virus had emerged and was co-circulating with the low pathogenicity strains.

Methods: Here we characterize the pathogenicity of a newly emerged human H7N9 variant with a PEVPKRKRTAR/GLF insertion motif at the cleavage site of the HA protein *in vitro* and *in vivo*.

Results: This variant replicates in MDCK cells independently of TPCK-trypsin, which is indicative of high pathogenicity in chickens. The 50% mouse lethal dose (MLD_{50}) of this novel isolate was less than 10 plaque forming units (PFU), compared with 3.16×10^4 for an identical virus lacking the polybasic insertion, indicating a high virulence phenotype.

Conclusions: Our results demonstrate that the multiple basic amino acid insertion in the HA protein of the H7N9 variant confers high virulence in mammals, highlighting a potential risk to humans. Continuous viral surveillance is therefore necessary in the China region to improve pandemic preparedness.

Keywords: Influenza A virus (IAV); H7N9; highly pathogenic avian influenza (HPAI); polybasic connecting peptide; cleavage site

Submitted Feb 04, 2021. Accepted for publication Jun 18, 2021.
doi: 10.21037/jtd-21-226
View this article at: https://dx.doi.org/10.21037/jtd-21-226

[†] Present address: Weill Cornell Medicine, xih4001@med.cornell.edu.

[‡] Present address: St. Jude Children's Research Hospital, min.zheng@stjude.org.

Introduction

Influenza A virus (IAV) infects a variety of avian and mammalian hosts. Human IAV is a major respiratory disease affecting a broad range of the population each year. Pandemic H1N1 (pdmH1N1/2009) and H3N2 subtypes currently co-circulate with type B viruses worldwide (1). In addition, many terrestrial poultry species can be infected by avian IAV. Generally, mammalian and avian IAVs circulate only in their own hosts due to host restriction factors, although some avian viruses, such as H5N1, H7N9, H10N8, and H5N6 subtype viruses, may occasionally cross species barriers, being sporadically transmitted from domestic poultry to humans or other mammalian hosts. There is concern that avian influenza viruses like these might acquire adaptative mutations conferring sustainable mammalian transmissibility due to selective pressure from the host immune system (2). In 1997, highly pathogenic avian influenza (HPAI) H5N1 was the first avian subtype to cause human fatalities. Fortunately, its genetic composition, isolated from humans, has remained wholly of avian origin and these viruses are poorly transmitted among humans (3).

In early 2013, avian H7N9 subtype IAV first infected humans, causing fatalities in eastern China (4). Up to now, more than 1,500 human cases have been reported by the Food and Agriculture Organization of the United Nations (http://www.fao.org/ag/againfo/programmes/en/empres/h7n9/situation_update.html). Most patients that contracted H7N9 virus suffered from primary viral pneumonia and in some severe cases, developed acute respiratory distress syndrome (ARDS) (4,5). Some of people experienced mild or asymptomatic outcomes after being infected with H7N9 virus (6,7). Epidemiological data demonstrated that avian H7N9 viruses generally more readily infected humans than did other avian influenza subtype viruses, such as H5N1 and H9N2. Thus, there is concern that the H7N9 virus may further adapt in humans, gaining new genetic features to become more pathogenic (8).

The polybasic peptide between HA1 and HA2 acts as a key virulence marker in H5 and H7 subtype influenza viruses (9). This motif is a hallmark of highly pathogenic strains of type A influenza viruses and confers lethality in chickens. However, the level of virulence does not correspond with particular polybasic peptide sequences (10). Collective studies have demonstrated that the key markers for avian influenza virus virulence in mammalian hosts are mainly located within the PB2 protein, such as E627K and D701N (11). Our previous study characterized an H7N9 human isolate (A/Zhejiang/DTID-ZJU01/2013, ZJ1), which contained a mammalian adaptation biomarker, PB2 701N. The patient was leucopenic and lymphopenic, and had impaired liver and renal function, substantially increased serum cytokine and chemokine concentrations, and disseminated intravascular coagulation with disease progression (4). The original 2013 H7N9 virus lacked the polybasic peptide, and viruses bearing the peptide did not emerge until the fifth wave of the outbreak, which started in mid-2016 (12). During this fifth wave of the epidemics, which continued until 15 April 2017, there were a total of 517 laboratory-confirmed cases, with 186 patient deaths (13). An H7N9 virus possessing the polybasic peptide was isolated from the trachea of a 56-year-old patient with diabetes and hypertension in 2017 (14). The highly pathogenic human H7N9 isolate A/Qingyuan/GIRD1/2017 (QY) used in the present study was isolated from endotracheal aspirate collected from the same patient on day 9 of their illness, and is therefore genetically similar to the A/Guangdong/17SF006/2017 isolate described in the above study. Although both of these viruses were sourced from the same patient, virus isolation, propagation, genome assembly and sequence submission were performed independently by two different research groups. In the present study, we characterize the general biological properties of the QY strain using in-vitro and in-vivo approaches.

We present the following article in accordance with the ARRIVE reporting checklist (available at https://dx.doi.org/10.21037/jtd-21-226).

Methods

Viruses and cells

The full genome sequences were determined by the Sanger Sequencing Method and dominant sequences were exported as the reference sequences for recombination of QY WT and mutant viruses. All recombinant influenza viruses used in this study were generated using the reverse genetics (RG) technique to ensure the absence of contamination from other microbes and unwanted mutations. RG viruses were propagated in 10-day-old specific pathogen-free (SPF) embryonated chicken eggs (P1), using a standard protocol approved by the University of Hong Kong Committee on the Use of Live Animals in Teaching & Research (CULATR #4351-17). All P1 viruses were confirmed by sequencing and titrated by plaque assay using Madin-Darby canine

Table 1 Genotypes of recombinant influenza A viruses used in this study

Virus abbreviation	PB2	PB1	PA	NP	HA	NA	M	NS
QY WT	QY	QY	QY	QY	QY	QY	QY	QY
QY HAΔ	QY	QY	QY	QY	QYΔ	QY	QY	QY
QY + ZJ1-HA	QY	QY	QY	QY	ZJ1	QY	QY	QY
ZJ1	ZJ1	ZJ1	ZJ1	ZJ1	ZJ1	ZJ1	ZJ1	ZJ1
ZJ1 + HAΔ	ZJ1	ZJ1	ZJ1	ZJ1	QYΔ	ZJ1	ZJ1	ZJ1

kidney (MDCK) cells [American Type Culture Collection (ATCC)]. MDCK cells were maintained in Eagle's minimal essential medium (MEM, Invitrogen). A549 human cells (ATCC) and DF-1 chicken fibroblast cells were maintained in Dulbecco's modified essential medium (DMEM, Invitrogen). All culture media contained 10% fetal bovine serum (FBS, Invitrogen) and 1% penicillin and streptomycin. Cells were incubated at 37 ℃ and supplied with 5% CO_2. All experiments involving H7N9 viruses were performed in bio-safety level 3 (BSL3) laboratories at the University of Hong Kong, following standard operational protocols.

Viral genome characterization and RG

Viral RNA was extracted from cell cultures or allantoic fluid using the QIAamp® Viral RNA Mini Kit (Qiagen) and cDNA was transcribed using SuperScript III Reverse Transcriptase (Invitrogen). Briefly, viral segments were cloned into the pHKU_FluA plasmid system, a derivation of the pHW2000 plasmid system containing both Pol I and Pol II promoters flanking a Stuff segment (around 1.7kbp) that ends with highly conserved IAV Uni12 and Uni13 termini (Figure S1) (protocol is available upon request). A QY HA lacking the polybasic connecting peptide (HAΔ) was generated by inverse PCR (Figure S2). Another H7N9 strain, A/Zhejiang/DTID-ZJU01/2013 (ZJ1), was also used in this study (4). The QY strain was used as a backbone to rescue wild type (QY WT), recombine with HAΔ (QY HAΔ), and reassort with ZJ1 HA (QY + ZJ1-HA). The QY HAΔ segment was also reassorted with the ZJ1 backbone to generate ZJ1 + HAΔ. A total of five different recombinant viruses were used in this study (*Table 1*) (15,16).

Virus genomes

The full genome sequence of the A/Qingyuan/GIRD1/2017 virus used in this study is deposited in Genbank (Accession numbers KY621539 to KY621546); Genbank accession numbers for A/Zhejiang/DTID-ZJU01/2013 are KC885955 to KC885962.

Trypsin dependent assay

Confluent MDCK monolayers were infected with RG viruses at a multiplicity of infection (MOI) of 5. The viral inoculums were removed after one hour of adsorption at 37 ℃ and replaced with MEM with or without TPCK-trypsin (1 μg/mL). Infected cells were then incubated at 37 ℃, supplied with 5% CO_2. Supernatant was collected at 8 hours post-infection, followed by immunoblotting using anti-HA polyclonal antibody against the HA2 fragment (a gift from Dr. Yixin Chen, Xiamen University).

Growth kinetics of virus in cells

Confluent MDCK cells were infected with RG viruses at an MOI of 0.001. The viral inoculums were removed after an hour's adsorption at 37 ℃ and replaced with MEM containing 1 μg/mL of TPCK-trypsin. The cells were further incubated at 37 ℃, with 5% CO_2. Culture supernatants were collected at different post-infection time points. Confluent A549 or DF-1 cells were infected with RG viruses at an MOI of 0.01. The viral inoculums were removed after one hour's adsorption at 37 ℃; cells were then washed using MEM and overlaid with MEM containing 1 μg/mL of TPCK-trypsin. Infected cells were further incubated at 37 ℃, supplied with 5% CO_2. Culture supernatants were collected at different time points after infection. Ten-day-old SPF embryonated chicken eggs were inoculated with 100 PFU of the RG viruses and cultured at 37 ℃. Allantoic fluid was collected at three different time points following infection. Virus titers were determined by standard plaque assay in MDCK cells.

Table 2 Comparison of HA segment amino acids between QY and ZJ1 strains

	56	130	136	143	182	186	235*	245	335	340	400	407	503
QY	T	P	N	V	E	I	Q	I	V	RKRTA	A	K	R
ZJ1	I	A	S	A	K	L	L	M	I	----G	E	E	S

Numbering starts from methionine, including a 16-aa signal peptide. *, HA 226 receptor binding site (H3 numbering).

Mouse experiments

In total, 55 BALB/c mice, aged 6–8 weeks and weighted around 20 g, were obtained from the University of Hong Kong Laboratory Animal Unit. Fifty mice were randomly grouped into five groups which were anesthetized with isoflurane (Halocarbon Laboratory), and inoculated intranasally with 10^1, 10^2, 10^3, 10^4, or 10^5 PFU (25 µL) of QY WT or QY HAΔ RG virus. Animals in the control group were inoculated intranasally with 25 µL of PBS. Animals were observed daily for mortality and body weight was measured for up to 14 days after infection. The median mouse lethal dose (MLD_{50}) was calculated using the Reed and Muench method (17). The risk assessment for this study was approved by the Safety Committee on BSL-3 Facility and Infectious Agents, Li Ka Shing Faculty of Medicine, the University of Hong Kong. The protocols for animal experiments and the use of embryonated chicken eggs (9–11 days old) were approved by the CULATR, Li Ka Shing Faculty of Medicine, the University of Hong Kong (CULATR #4351-17). The CULATR follows Hong Kong legislation and AAALAC recommended standards/guidelines (http://www.aaalac.org/about/guidelines.cfm).

Statistical analysis

GraphPad Prism ver. 8.02 for Windows (GraphPad Software, USA) was used to analyze the data. Two-way ANOVA was performed. Probability values of less than 0.01 ($P<0.05$) were considered statistically significant. No samples were excluded from the analysis.

Results

Molecular characterization

HA is a critical determinant of the pathogenicity of avian IAVs, with a clear link between HA cleavability and virulence (18). Generally, the HA proteins of highly pathogenic H5 and H7 viruses contain a multiple basic peptide between HA1 and HA2 (Figure S3). In this study, sequence analysis showed that the QY human isolate contained a multibasic connecting peptide (PEVP*KRKRTAR*/GLF) at the cleavage site of the hemagglutinin (HA) protein, indicating that it is a highly pathogenic strain (Figure S2). This type of motif, which includes PEVP*KRKRTAR*/GLF as well as PEVP*KGKRIAR*/GLF, was first identified in the fifth wave of H7N9 human infections. Glutamine was observed at amino acid position 226 (H3 numbering) on the HA, which suggested that the QY strain prefers binding to α-2,3-sialic acid receptors on the cell membrane. The genotype of QY HA del used in this study was PEIPKGR/GLF. Besides the multibasic connecting peptide, the QY strain has an additional 12 amino acid differences from the HA of the ZJ1 virus (*Table 2*), indicating that H7N9 viruses are undergoing continuous evolution to escape the host immune system.

The H7N9 PB2 substitution E627K was frequently observed in human isolates after the outbreak in 2013. We amplified a partial sequence of the PB2 gene to generate a TA clone library to verify from the clinical sample whether the patient had been infected with an avian strain. In total, we screened 34 PB2 plasmids and found the E:K ratio to be 8:26, indicating that this isolate was originally from poultry and that the PB2 E627K substitution had appeared rapidly after infection (data not shown).

Although sequencing assembly data showed that the NA R292K (N2 numbering) residue was conferred resistance to oseltamivir [a neuraminidase (NA) inhibitor], it was possible that the endotracheal isolate contained oseltamivir sensitive genotype virus. To calculate the mutation ratio, 84 TA clones of NA genes were sequenced and the R:K ratio at position 292 found to be 16:68 (≈1:4), indicating that lysine became dominant after the patient was treated with oseltamivir (data not shown).

Trypsin independent replication of QY in MDCK cells

To test whether QY WT, which has a HA polybasic connecting peptide, can replicate independently of TPCK-trypsin in mammalian cells, a single cycle infection assay

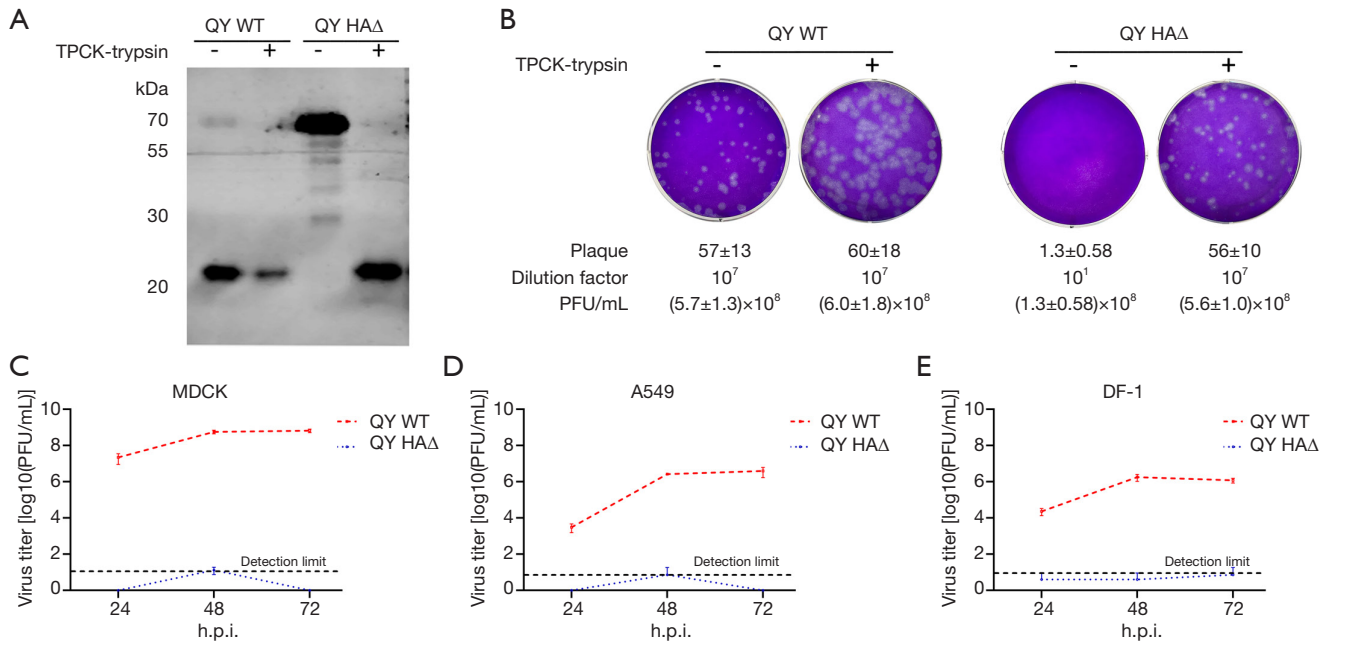

Figure 1 Trypsin dependency analysis. A/Qingyuan/GIRD1/2017 (QY WT) and HA multiple basic peptide deletion mutant (QY HAΔ) were rescued by reverse genetics (RG). (A) both RG viruses (MOI =5) were inoculated onto confluent MDCK cells with or without treatment with TPCK-trypsin (1 μg/mL). Virus-infected cells were collected at 8 h post infection (h. p. i.) and immunoblotted using anti-HA polyclonal antibody. (B) QY WT and HAΔ viruses were inoculated onto MDCK cells with or without treatment with TPCK-trypsin and fixed at 48 h post-infection. Plaques were stained using 0.5% crystal violet. QY WT and HAΔ RG viruses were used to infect (C) MDCK cells at 0.001 MOI, (D) A549 cells at 0.01 MOI, and (E) DF-1 cells at 0.01 MOI, without TPCK-trypsin treatment. The cells were cultured at 37 ℃ and supernatants collected at 24, 48, and 72 h post infection and subjected to plaque assays in MDCK cells to determine virus titers. Error bars represent mean ± s.d. (n=3, biological replicates).

(MOI =5) was used, with MDCK cells being infected with QY WT and QY HAΔ, followed by immunoblotting with an HA2-specific polyclonal antibody. The majority of the QY WT HA detected was the HA2 segment (which contains the PEVPKRKRTAR/GLF motif), indicating that cleavage occurred independently of TPCK-trypsin (*Figure 1A*, lane 1). However, the QY HAΔ segment was visible around 70 kDa, suggesting that it was not cleaved into two parts without TPCK-trypsin (*Figure 1A*, lane 3). Both RG virus HA segments were cut into two fragments following treatment with TPCK-trypsin, so that only HA2 fragments were visible (*Figure 1A*, lanes 2 and 4). Next, we quantitated viral plaques in the absence or presence of TPCK-trypsin. All the viral particles were inoculated at 100 PFU onto MDCK monolayers and fixed at 48 h post-infection. In the absence of TPCK-trypsin, QY WT formed $(5.7±1.3)×10^8$ PFU/mL, but QY HAΔ only formed 13±5.8 plaques/mL, which was under the detection limit (*Figure 1B*, wells 1 and 3, *Figure 1C* 48 h. p. i. time point). In the presence of TPCK-trypsin, both QY WT and QY HAΔ formed close numbers of plaques The number of plaques formed was comparable in the presence of TPCK-trypsin (*Figure 1B*, wells 2 and 4). Additionally, the size of plaques formed by viruses treated with TPCK-trypsin was larger than that of virus cultures free of TPCK-trypsin, indicating that the HA is not cleaved very efficiently by furin or other endogenous proprotein convertases in MDCK cells. This might be due to the minimal furin recognition motif of the cleavage site: R-X-X-R lacking a basic amino acid in position P2 (*Figure 1B*, wells 1 and 2). Growth kinetics results showed that this novel human isolate can replicate trypsin-independently in MDCK, A549 and DF-1 cells. However, neither of the three cell lines supported growth of the RG virus with HAΔ genotype (*Figure 1C-1E*). In summary, the novel QY H7N9 strain can propagate independently without the assistance of TPCK-trypsin. Like HPAI H5N1 subtypes, it might be able to replicate ubiquitously by utilizing intracellular

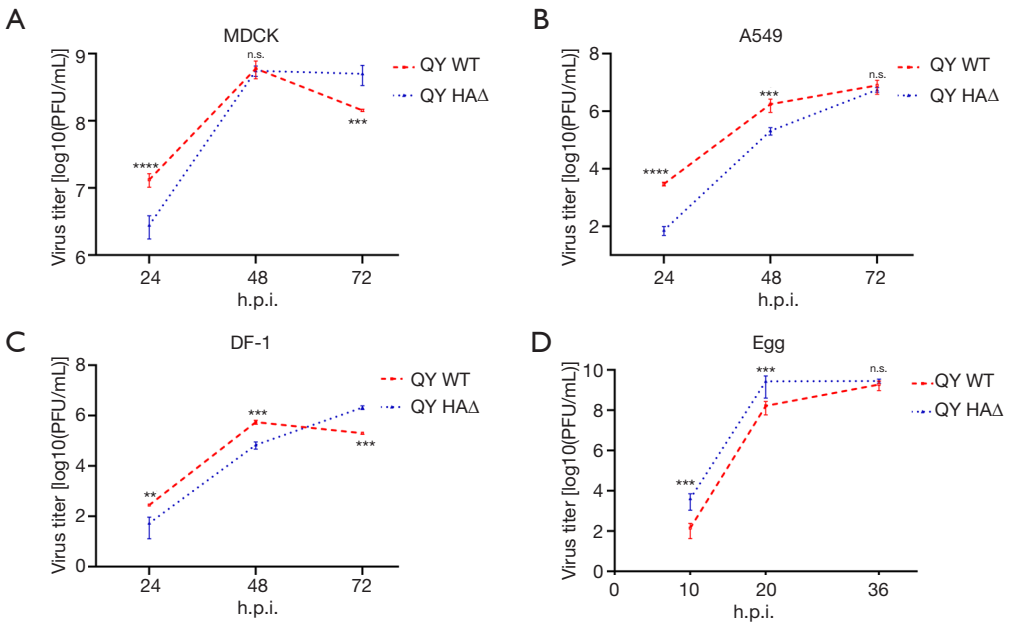

Figure 2 Growth kinetics of QY WT and HAΔ viruses in mammalian cells, avian cells and in ovo. WT and HAΔ RG viruses were used to infect (A) MDCK cells at 0.001 MOI, (B) A549 cells at 0.01 MOI, and (C) DF-1 cells at 0.01 MOI, all with TPCK-trypsin treatment (1 μg/mL). The cells were cultured at 37 ℃ and supernatants collected at 24, 48, and 72 h post infection and subjected to plaque assays in MDCK cells to determine virus titers. (D) Ten-day-old SPF chicken eggs were inoculated with 100 PFU of the RG viruses and cultured at 37 ℃. Allantoic fluid was collected at 10, 20, and 35 h post infection. Virus titers were determined by standard plaque assay in MDCK cells in this study. Error bars represent mean ± s.d. (n=3, biological replicates). Statistical significance was analyzed by two-way ANOVA on the log-transformed data, followed by Sidak's test: **, P<0.01; ***, P<0.001; ****, P<0.0001. n. s., no significance; h. p. i., hours post infection.

proteases such as furin and PC6, rather than relying on proteases present in the respiratory tract (19).

Growth kinetics

QY WT possessed a growth advantage in MDCK, A549 and DF-1 cells (*Figure 2A-2C*). The data rather show that QY WT replicates efficiently in DF-1 and MDCK cells and has reached its peak titer already at 48 h. p. i.. However, QY WT did not demonstrate the advantage compared to QY HAΔ, indicating that the virus is still clearly an avian virus with primary spread in wild and domestic bird populations and that acquisition of a polybasic connecting peptide by H7 subtype viruses is relatively frequently associated outbreaks in birds (*Figure 2D*). Humans and other mammals remain largely dead-end hosts so are much less likely to act efficiently as adaptation hosts.

Pathogenicity in mice

To further examine the effect of the HA polybasic connecting peptide *in vivo*, RG virions of QY WT and QY HAΔ viruses were tested in a SPF-mouse infection model.

We first estimated the 50% mouse lethal dose (MLD_{50}) of both RG viruses. Groups of five mice were anesthetized with isoflurane (Halocarbon Laboratory), and inoculated intranasally with 10^1, 10^2, 10^3, 10^4, or 10^5 PFU (25 μL) of QY WT or QY HAΔ RG virus. Our results showed that inclusion of the polybasic connecting peptide increased mortality in infected mice. The 50% mouse lethal dose (MLD_{50}) of QY WT cannot be determined by those five dosages, even 10 PFU still caused 100% lethal the mice. Therefore, the MLD_{50} of QY WT was less than 10 PFU. However, QY HAΔ's was 3.16×10^4 PFU, which is similar to that of the first H7N9 strain to infect humans isolated in 2013 (16) (*Figure 3A-3F*). The body weight loss assay results showed that QY WT caused severe body weight loss or lethality to mice in all five dosage groups. However, only the highest dosage (10^5 PFU/25 μL) of QY HAΔ resulted in mouse death, while the four groups inoculated with lower doses of QY HAΔ (less than 10^4 PFU/25 μL) did not experience apparent loss of body weight, when

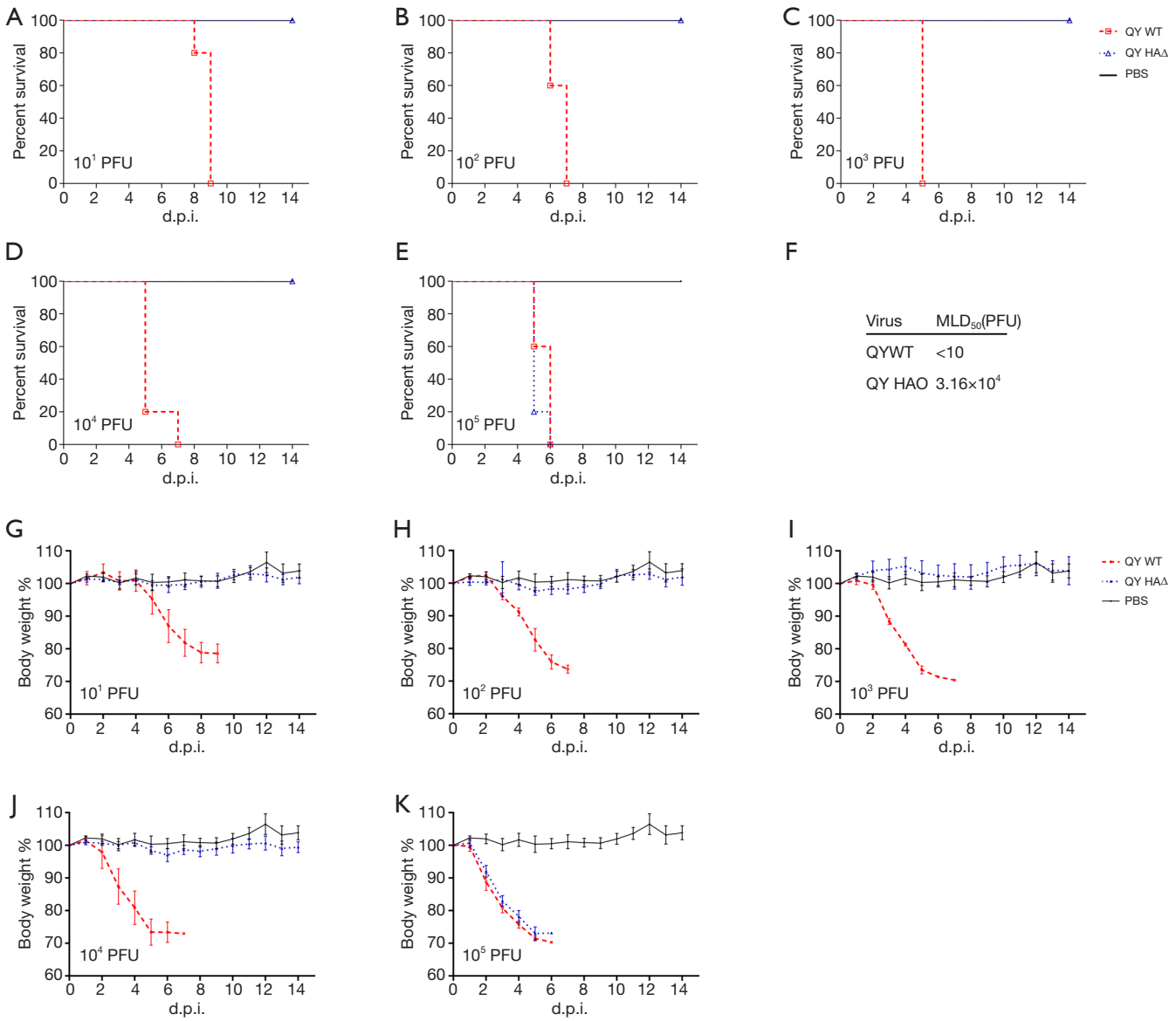

Figure 3 Mouse pathogenicity analysis. Groups of 6- to 8-week-old female BALB/c mice were infected with 25μl inoculums containing 10^1, 10^2, 10^3, 10^4 or 10^5 PFU of RG versions of viruses or PBS control, as specified. Mice were observed daily for changes in body weight for 14 days (day 0 to day 14). Animals that lost over 25% of their pre-infection weight were euthanized, in accordance with our institutional animal ethics guidelines. The MLD_{50} values were calculated according to the standard method. Error bars represent mean ± s.e.m. (n=5).

compared with the phosphate-buffered saline (PBS) control (*Figure 3G-3K*). These results confirm that the HA multibasic connecting peptide is a highly pathogenic factor in mammals.

Difference of ZJ1 and QY H7N9

To investigate the effect of other HA residues, another two RG viruses using (I) QY as the backbone and incorporating ZJ1 HA, or (II) ZJ1 as the backbone and including QY HAΔ were generated. These viruses were paired with similar backbone RG viruses that differed in the HA and used to inoculate eggs or infect MDCK or A549 cells (*Figure 4A-4F*). Growth kinetics data showed that for both pairs of RG viruses, those with the QY HAΔ segment replicated faster than those with ZJ1 HA,

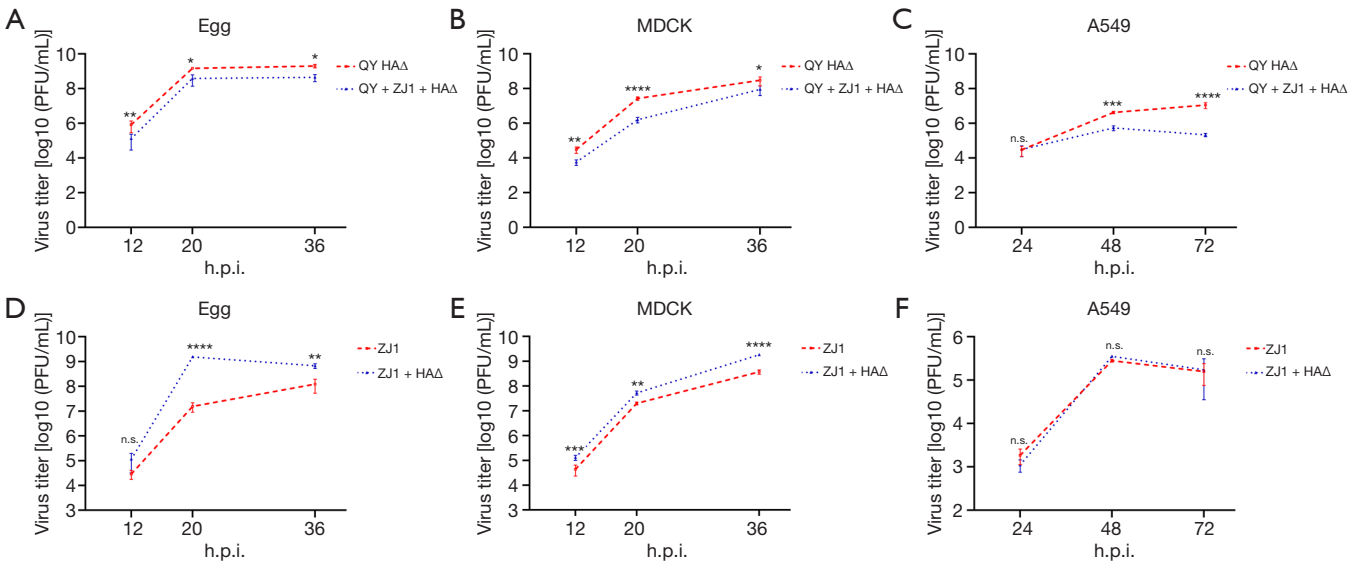

Figure 4 Growth kinetics of H7N9 viruses carrying different HA variants in embryonated chicken eggs and mammalian cells. Reverse genetic versions of QY viruses carrying HAΔ or ZJ1-HA were used to infect (A) ten-day-old embryonated chicken eggs with 100 PFU of the respective viruses, (B) MDCK cells at an MOI of 0.001, and (C) A549 cells at an MOI of 0.01. Reverse genetic versions of H7N9/ZJ1 viruses carrying ZJ1-HA or HAΔ were used to infect (D) ten-day-old embryonated chicken eggs with 100 PFU of the respective viruses, (E) MDCK cells at an MOI of 0.001, and (F) A549 cells at an MOI of 0.01. All cell cultures were supplemented with TPCK-trypsin (1 μg/mL). Allantoic fluid or culture supernatants were harvested at the indicated time points and viruses titrated by plaque assay. Error bars represent mean ± s.d. (n=3, biological replicates). Statistical significance was analyzed by two-way ANOVA on the log-transformed data, followed by Sidak's test: *, P<0.05; **, P<0.01; ***, P<0.001; ****, P<0.0001. n.s., no significance; h.p.i., hours post infection.

suggesting that the ZJ1 HA behaves differently with the QY HAΔ.

Discussion

Here, we have characterized the virulence of a novel H7N9 virus isolated from a fatal human case. The virus carries multiple basic amino acids in the connecting peptide of the HA, making it lethal to mice in a low viral titer (less than 10 PFU). While previously circulating strains contained a single arginine residue at the cleavage site of HA, this novel virus has acquired a polybasic cleavage site within the HA. Similar insertions have also been identified in the HA sequences of several human and poultry H7N9 isolates collected in Guangdong province since early 2017 (20). Chan *et al.* demonstrated that this HPAI-H7N9 was more efficient at replicating in human alveolar epithelial cells and pulmonary microvascular endothelial cells than LPAI-H7N9 implying that endothelial tropism may involve in pathogenesis of HPAI-H7N9 disease (21). Interestingly, an H7N9 HA sequence detected from an environmental sample (A/Environment/Guangdong/C16283222/2016) contains an insertion and has a highly similar sequence, but it lacks a mutation from glycine to arginine at the cleavage site (14). This implies that the new H7N9 strain may have potentially emerged in this area, although more evidence, especially the direct isolation of such viruses from poultry, is needed to support this conclusion.

These viruses have the potential to grow vigorously within the host due to their polybasic motifs, which enhance their replication *in vivo* (22). To date, only H5 and H7 subtypes have been observed to possess such motifs, with a diverse variety of motif genotypes being identified. Cleavage sites can contain one or more non-basic amino acids (Figure S3). Prior to 2013, it was reported that the H7N x isolates (NA subtypes include N1, N3, N4, N7, N8, and N9) have resulted in over 100 cases of human infection since 2002 the Netherlands, Italy, the United Kingdom, Canada, and the United States (23), but no human cases infected with a HA polybasic connecting peptide was reported. Investigating how the polybasic cleavage site appeared, Stech *et al.* reported that a reassortant H7N8 influenza

virus which was derived from an H3N8 backbone strain (A/duck/Ukraine/1/1963) and contained an H7 gene from an H7N7 isolate (A/chicken/Germany/R28/2003) gained high pathogenicity associated cleavage sites (PEIP*KRRRR*/GLF) following serial passage in vitro. Only ten percent of SPF chickens showed symptoms of illness after infection with this recombinant strain, suggesting that the multiple basic connecting peptide might not be uniquely responsible for pathogenicity in chickens (24). Since the reassortant was not a natural isolate, it is possible that the engineered HA-NA combination might have undermined viral fitness in chickens, despite the presence of an HA containing a multibasic peptide (25). Scheibner *et al.* reported on another H7N7 isolate whose polybasic peptide, unlike that of the QY isolate, lacked threonine and alanine (PEIP*KRKRR*/GLF). This genotype displayed high pathogenicity in chickens and turkeys, but not in Peking and Mallard ducks (26). Qi *et al.* reported similar results in a study of 2017 H7N9 isolates (27). Sun *et al.* also characterized a reassortant HPAI H7N9 strain (TW/17) with a polybasic mutation genotype (PEVP*KGKR*TA*R*/GLF), using PR8 internal genes as the backbone. Lung titers following a lower dosage inoculation were significantly increased in mice, indicating that this virus could replicate effectively in the mouse lung. Interestingly, the virus did not propagate well when inoculated at a higher dosage (28). Infection with the natural H7N9 (TW/17) strain also resulted in severe symptoms in ferrets (29). In summary, H7N9 viruses with multiple basic amino acids at the HA cleavage site generally cause severe infections in both terrestrial poultry and mammals.

Nao *et al.* elucidated a possible mechanism in which the polybasic connecting peptide within the H5 or H7 segment is acquired through evolution from a low-pathogenicity precursor, which contains an RNA stem-loop structure (30). H7N9 subtypes with polybasic cleavage sites did not appear until the fifth wave of the outbreak in China in mid-2016. In this study, we identified that, besides the multiple basic peptide (PEVP*KRKR*TA*R*/GLF), there are 12 amino acid differences between QY and ZJ1 HA, one of which is in the HA receptor binding region required for efficient infection. QY has partially acquired the mammalian adaptation biomarker, having G186V on the 190 helix, but is still unchanged on the 220 loop (226L). Moreover, two reassortant viruses carrying the QY HAΔ grew faster than viruses with an identical backbone, but carrying ZJ1 HA, both *in ovo* and in mammalian cells (*Figure 4*), suggesting that the QY strain is better adapted for more efficient replication in host species and that one or more of the twelve amino acids that differ between the HA proteins of the two strains might increase QY virulence beyond that conferred by the polybasic connecting peptide. It has been reported that HA2-K64 is a biomarker contributing to high virulence independently of the multiple basic cleavage site (28). A systematic study to compare pathogenic differences using a series of reassortant viruses might give us a better understanding of the evolution of the H7N9 HA segment from low to high pathogenicity.

Since the QY strain was isolated from the patient on day 9 following disease onset, mammalian substitutions (PB2 E627K) were observed in the virus during the preceding days of infection. PB2 E627K is a mammalian adaptation signature which affects viral pathogenicity in the host, whereas avian isolates prefer glutamine (glu, E) at that position. Interestingly, PB2 K526R, D701N and Q591K mutations were also found in other isolates from the fifth wave of the outbreak that contained polybasic connecting peptides (20,31). The diversity of PB2 substitution has persisted in H7N9 since its outbreak in 2013.

Given that the majority of H7N9 viruses are already resistant to amantadine, the occurrence of additional mutations conferring oseltamivir resistance remains a public concern. The NA R292K mutation was previously identified in some isolates from patients infected with H7N9 and it was suggested to associate with prolonged virus shedding and adverse clinical outcomes (32,33). It is not yet well understood if the polybasic cleavage site in the H7N9 virus may influence the selection of NA R292K. Studies of H5N1 viruses have demonstrated that viruses with either polybasic residues in the HA or the E627K mutation in PB2 have enhanced replication efficiency both *in vitro* and *in vivo* (34,35). While the newly identified QY H7N9 strain has obtained both an HA polybasic connecting peptide and the E627K mutation, whether these two factors contributed to the selection process under the pressure of oseltamivir treatment still requires further investigation.

The avian H7N9 virus has been endemic in China since 2013 and has caused five waves of outbreaks. Although there is still limited information regarding the impact of the H7N9 virus following the acquisition of the polybasic cleavage site in the HA, we here show that this virus is highly pathogenic, and that infection could potentially lead to severe clinical outcomes. This widespread and rapidly evolving virus lineage thus poses a considerable threat to human health.

Acknowledgments

We are grateful to Dr. Jane Rayner for editing the manuscript.

Funding: This work was supported by the General Project of Guangzhou Medical University (Grant No. SKLRD-MS-201908), the National Natural Science Foundation of China (Grant No. 82074311), Yunnan Provincial Science and Technology Department (No. 202005AF150043), Guangzhou Institute of Respiratory Health Open Project (Funds provided by China Evergrande Group, Project No. 2020GIRHHMS18), and the Research Grants Council of the Hong Kong SAR (Grant No. 17103214, 17154516 and 17107019).

Footnote

Reporting Checklist: All authors have completed the ARRIVE reporting checklist. Available at https://dx.doi.org/10.21037/jtd-21-226

Data Sharing Statement: Available at https://dx.doi.org/10.21037/jtd-21-226

Peer Review File: Available at https://dx.doi.org/10.21037/jtd-21-226

Conflicts of Interest: All authors have completed the ICMJE uniform disclosure form (available at https://dx.doi.org/10.21037/jtd-21-226). The authors have no conflicts of interest to declare.

Ethical Statement: The authors are accountable for all aspects of the work in ensuring that questions related to the accuracy or integrity of any part of the work are appropriately investigated and resolved. The protocols for animal experiments and the use of embryonated chicken eggs (9-11 days old) were approved by the CULATR, Li Ka Shing Faculty of Medicine, the University of Hong Kong (CULATR #4351-17). The CULATR follows Hong Kong legislation and AAALAC recommended standards/guidelines (http://www.aaalac.org/about/guidelines.cfm).

References

1. Phipps KL, Marshall N, Tao H, et al. Seasonal H3N2 and 2009 Pandemic H1N1 Influenza A Viruses Reassort Efficiently but Produce Attenuated Progeny. J Virol 2017;91:e00830-17.
2. Taubenberger JK, Kash JC. Influenza virus evolution, host adaptation, and pandemic formation. Cell Host Microbe 2010;7:440-51.
3. Chen H, Smith GJ, Zhang SY, et al. Avian flu: H5N1 virus outbreak in migratory waterfowl. Nature 2005;436:191-2.
4. Chen Y, Liang W, Yang S, et al. Human infections with the emerging avian influenza A H7N9 virus from wet market poultry: clinical analysis and characterisation of viral genome. Lancet 2013;381:1916-25.
5. Gao R, Cao B, Hu Y, et al. Human infection with a novel avian-origin influenza A (H7N9) virus. N Engl J Med 2013;368:1888-97.
6. Yi L, Guan D, Kang M, et al. Family clusters of avian influenza A H7N9 virus infection in Guangdong Province, China. J Clin Microbiol 2015;53:22-8.
7. Chen Z, Liu H, Lu J, et al. Asymptomatic, mild, and severe influenza A(H7N9) virus infection in humans, Guangzhou, China. Emerg Infect Dis 2014;20:1535-40.
8. Westenius V, Mäkelä SM, Julkunen I, et al. Highly Pathogenic H5N1 Influenza A Virus Spreads Efficiently in Human Primary Monocyte-Derived Macrophages and Dendritic Cells. Front Immunol 2018;9:1664.
9. Govorkova EA, Rehg JE, Krauss S, et al. Lethality to ferrets of H5N1 influenza viruses isolated from humans and poultry in 2004. J Virol 2005;79:2191-8.
10. Abdelwhab EM, Veits J, Ulrich R, et al. Composition of the Hemagglutinin Polybasic Proteolytic Cleavage Motif Mediates Variable Virulence of H7N7 Avian Influenza Viruses. Sci Rep 2016;6:39505.
11. Steel J, Lowen AC, Mubareka S, et al. Transmission of influenza virus in a mammalian host is increased by PB2 amino acids 627K or 627E/701N. PLoS Pathog 2009;5:e1000252.
12. Quan C, Shi W, Yang Y, et al. New Threats from H7N9 Influenza Virus: Spread and Evolution of High- and Low-Pathogenicity Variants with High Genomic Diversity in Wave Five. J Virol 2018;92:e00301-18.

13. Su S, Gu M, Liu D, et al. Epidemiology, Evolution, and Pathogenesis of H7N9 Influenza Viruses in Five Epidemic Waves since 2013 in China. Trends Microbiol 2017;25:713-28.
14. Ke C, Mok CKP, Zhu W, et al. Human Infection with Highly Pathogenic Avian Influenza A(H7N9) Virus, China. Emerg Infect Dis 2017;23:1332-40.
15. Hoffmann E, Neumann G, Kawaoka Y, et al. A DNA transfection system for generation of influenza A virus from eight plasmids. Proc Natl Acad Sci U S A 2000;97:6108-13.
16. Song W, Wang P, Mok BW, et al. The K526R substitution in viral protein PB2 enhances the effects of E627K on influenza virus replication. Nat Commun 2014;5:5509.
17. Reed LJ, Muench H. A simple method of estimating fifty per cent endpoints. Oxford University Press, 1938:493-7.
18. Schrauwen EJ, Herfst S, Leijten LM, et al. The multibasic cleavage site in H5N1 virus is critical for systemic spread along the olfactory and hematogenous routes in ferrets. J Virol 2012;86:3975-84.
19. Horimoto T, Nakayama K, Smeekens SP, et al. Proprotein-processing endoproteases PC6 and furin both activate hemagglutinin of virulent avian influenza viruses. J Virol 1994;68:6074-8.
20. Wang N, Sun M, Wang W, et al. Avian Influenza (H7N9) Viruses Co-circulating among Chickens, Southern China. Emerg Infect Dis 2017;23:2100-2.
21. Chan LLY, Hui KPY, Kuok DIT, et al. Risk Assessment of the Tropism and Pathogenesis of the Highly Pathogenic Avian Influenza A/H7N9 Virus Using Ex Vivo and In Vitro Cultures of Human Respiratory Tract. J Infect Dis 2019;220:578-88.
22. Suguitan AL Jr, Matsuoka Y, Lau YF, et al. The multibasic cleavage site of the hemagglutinin of highly pathogenic A/Vietnam/1203/2004 (H5N1) avian influenza virus acts as a virulence factor in a host-specific manner in mammals. J Virol 2012;86:2706-14.
23. Belser JA, Bridges CB, Katz JM, et al. Past, present, and possible future human infection with influenza virus A subtype H7. Emerg Infect Dis 2009;15:859-65.
24. Stech O, Veits J, Weber S, et al. Acquisition of a polybasic hemagglutinin cleavage site by a low-pathogenic avian influenza virus is not sufficient for immediate transformation into a highly pathogenic strain. J Virol 2009;83:5864-8.
25. Wang X, Zeng Z, Zhang Z, et al. The Appropriate Combination of Hemagglutinin and Neuraminidase Prompts the Predominant H5N6 Highly Pathogenic Avian Influenza Virus in Birds. Front Microbiol 2018;9:1088.
26. Scheibner D, Ulrich R, Fatola OI, et al. Variable impact of the hemagglutinin polybasic cleavage site on virulence and pathogenesis of avian influenza H7N7 virus in chickens, turkeys and ducks. Sci Rep 2019;9:11556.
27. Qi W, Jia W, Liu D, et al. Emergence and Adaptation of a Novel Highly Pathogenic H7N9 Influenza Virus in Birds and Humans from a 2013 Human-Infecting Low-Pathogenic Ancestor. J Virol 2018;92:e00921-17.
28. Sun X, Belser JA, Yang H, et al. Identification of key hemagglutinin residues responsible for cleavage, acid stability, and virulence of fifth-wave highly pathogenic avian influenza A(H7N9) viruses. Virology 2019;535:232-40.
29. Sun X, Belser JA, Pappas C, et al. Risk Assessment of Fifth-Wave H7N9 Influenza A Viruses in Mammalian Models. J Virol 2018;93:e01740-18. Erratum in: J Virol 2019;93(13): PMID: 30305359; PMCID: PMC6288346.
30. Nao N, Yamagishi J, Miyamoto H, et al. Genetic Predisposition To Acquire a Polybasic Cleavage Site for Highly Pathogenic Avian Influenza Virus Hemagglutinin. mBio 2017;8:02298-16.
31. Yang L, Zhu W, Li X, et al. Genesis and Spread of Newly Emerged Highly Pathogenic H7N9 Avian Viruses in Mainland China. J Virol 2017;91:e01277-17.
32. Marjuki H, Mishin VP, Chesnokov AP, et al. Neuraminidase Mutations Conferring Resistance to Oseltamivir in Influenza A(H7N9) Viruses. J Virol 2015;89:5419-26.
33. Yang L, Xie J, Zhang Y, et al. Emergence of waterfowl-originated gene cassettes in HPAI H7N9 viruses caused severe human infection in Fujian, China. Influenza Other Respir Viruses 2019;13:496-503.
34. Claas EC, Osterhaus AD, van Beek R, et al. Human influenza A H5N1 virus related to a highly pathogenic avian influenza virus. Lancet 1998;351:472-7.
35. Long JS, Howard WA, Núñez A, et al. The effect of the PB2 mutation 627K on highly pathogenic H5N1 avian influenza virus is dependent on the virus lineage. J Virol 2013;87:9983-96.

Cite this article as: Song W, Huang X, Guan W, Chen P, Wang P, Zheng M, Li Z, Wang Y, Yang Z, Chen H, Wang X. Multiple basic amino acids in the cleavage site of H7N9 hemagglutinin contribute to high virulence in mice. J Thorac Dis 2021;13(8):4650-4660. doi: 10.21037/jtd-21-226

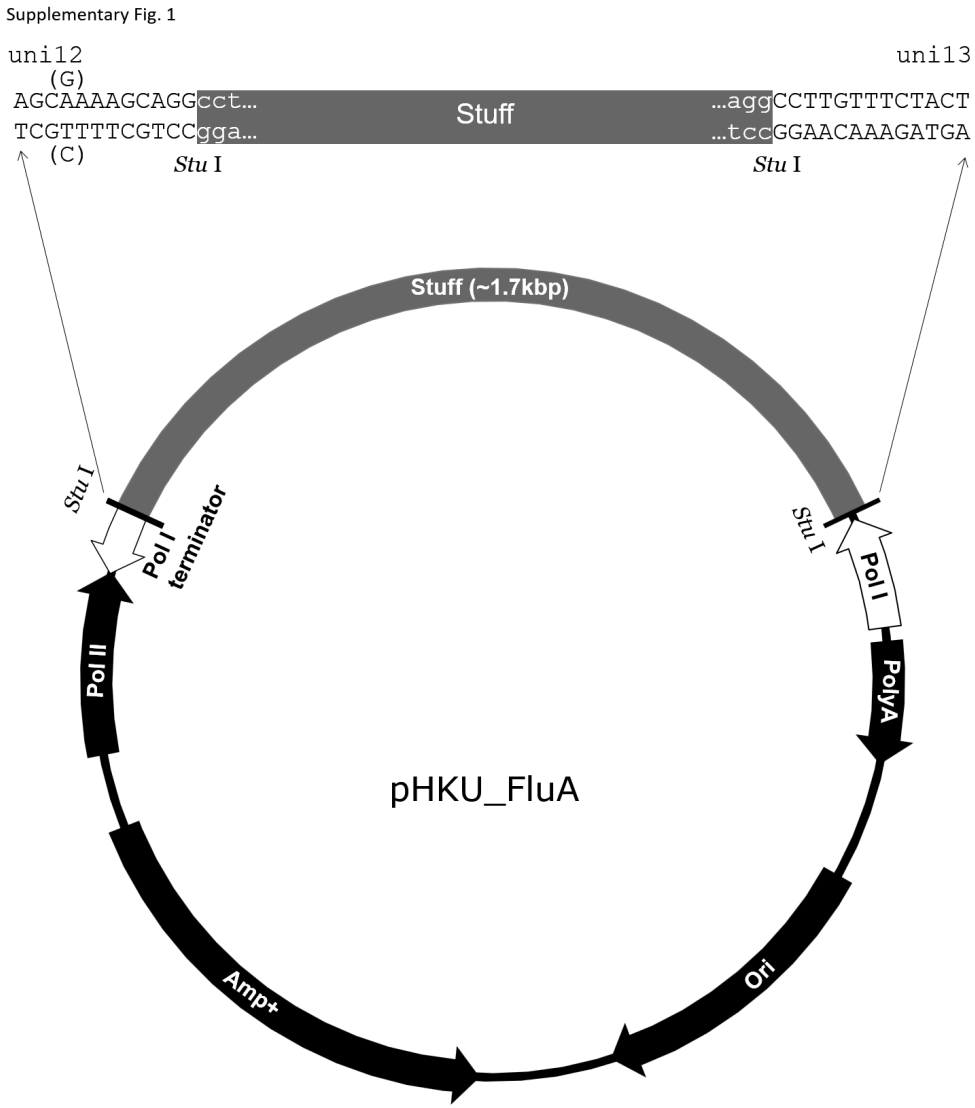

Figure S1 Physical map of the pHKU_FluA plasmid used as a backbone for construction of reverse genetic influenza A viruses in this study.

https://dx.doi.org/10.21037/jtd-21-226

Supplementary Fig. 2A HA alignment

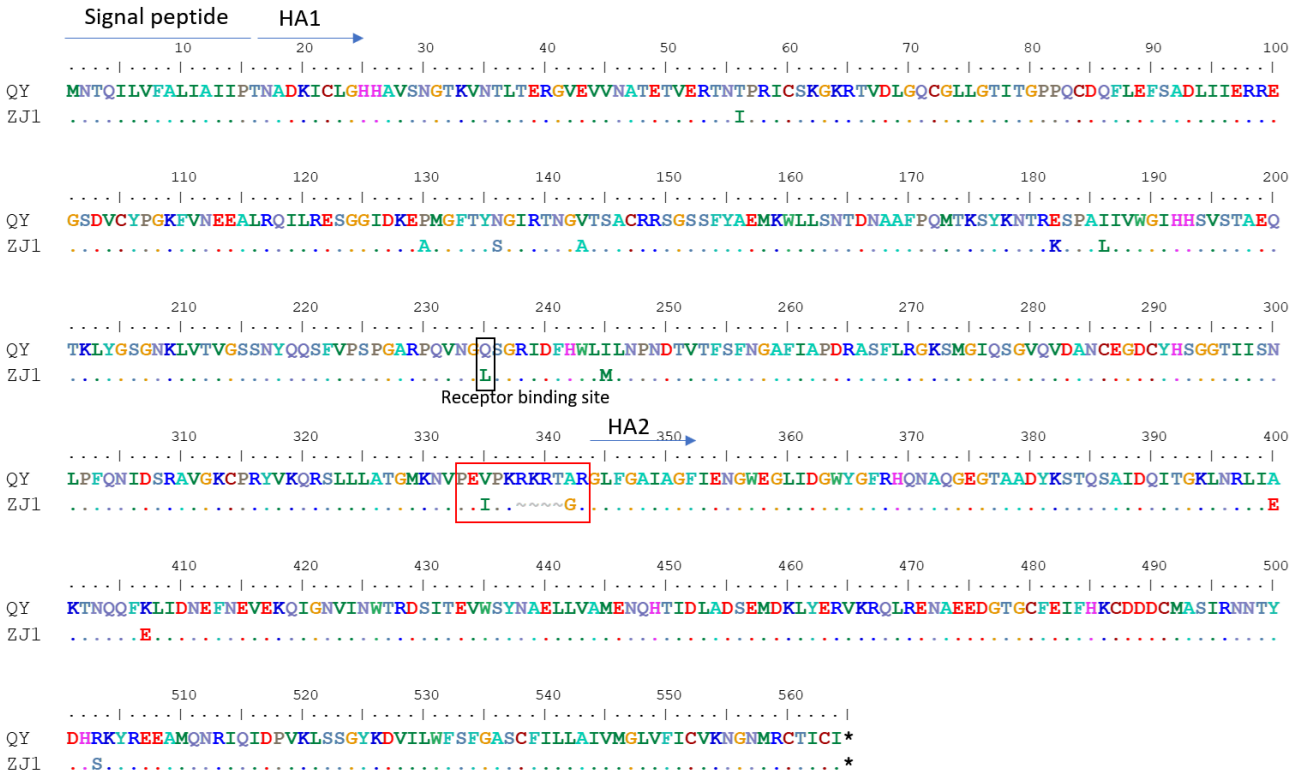

Supplementary Fig. 2B Reverse genetic viruses

Virus Sequence at HA cleavage site	
QY WT	PEVPKRKRTAR/G
QY HAΔ	PEIPK----GR/G
/, HA cleavage site	

Figure S2 HA sequence analysis and reverse genetics. (A) HA sequences from A/Qingyuan/GIRD1/2017 (H7N9) (QY) and A/Zhejiang/DTID-ZJU01/2013 (H7N9) (ZJ1) viruses are aligned. The black box indicates the HA receptor binding site (H3 numbering), and the red frame indicates the area that was engineered in the reverse genetic QY HAΔ virus. (B) Amino acid differences between QY WT and QY HAΔ.

https://dx.doi.org/10.21037/jtd-21-226

Subtype	Phenotype	Location	Year	Strain name	Cleavage site	Accession No.
H7	LP				PEIPKGR/GLF	
					PELPKGK/GLF	
					PEPPKGR/GLF	
					PENPKTR/GLF	
					PESPKTR/GLF	
H7N9	HP	China	2017	A/Qingyuan/GIRD1/2017	PEVPKRKRTAR/GLF	KY621542
				A/chicken/Guangdong/GD15/2016		EPI960361
				A/chicken/Guangdong/GD4/2017	PEVPKGKRTAR/GLF	KY855518
				A/Environment/Guangdong/C16283222/2016		EPI919615
				A/Guangdong/Th005/2017	PEVPKGKRIAR/GLF	EPI926825
H7N3	HP	Japan	2018	A/duck/Japan/AQ-HE30-1/2018	PEVPKRRRTAR/GLF	LC416566
H7N4	LP	China	2018	A/chicken/Jiangsu/1/2018	PELPKGR/GLF	EPI_ISL_332358
H7N9	HP	USA	2017	A/chicken/Tennessee/17-007147-2/2017	PENPKTDRKSRHRRIR/GLF	KY818811
H7N7	HP	Italy	2016	A/chicken/Italy/16VIR-1873/2016	PELPKGRKRR/GLF	EPI220955
H7N8	HP	USA	2016	A/turkey/Indiana/16-001403-1/2016	PENPKKRKTR/GLF	KU558906.1
H7N7	HP	UK	2015	A/chicken/England/26352/2015	PEIPRHRKGR/GLF	EPI623939
H7N7	HP	Germany	2015	A/chicken/Germany/AR1385/2015	PEIPKRKRR/GLF	FLI
H7N7	HP	Italy	2013	A/chicken/Italy/13VIR4527_11/2013	PETPKRRERR/GLF	KF569186.1
H7N3	HP	Mexico	2012-2018	A/chicken/Jalisco/CPA1/2012	PENPKDRKSRHRRTR/GLF	JX397993.1
				A/chicken/Puebla/CPA-04451/2016	PENPKDRKNRHRRTR/GLF	KX351916.1
				A/chicken/Jalisco/CPA-01859/2016	PENPKGKKSRHRKTR/GLF	KX351892.1
H7N7	HP	Spain	2009	A/chicken/Spain/6279-2/2009	PELPKGTKPRPRR/GLF	GU121458.1
H7N7	HP	UK	2008	A/chicken/England/1158-11406/2008	PEIPKRKKR/GLF	FJ476173.1
H7N3	HP	Canada	2007	A/chicken/Saskatchewan/HR-00011/2007	PENPKTTKPRPRR/GLF	EU500860.1
H7N7	HP	North Korea	2005	A/chicken/North Korea/1/2005	PEIPKGRHRRPKR/GLF	
H7N3	HP	Canada	2004	A/chicken/Canada/rv504/2004	PENPKQAYRKRMTR/GLF	CY015006.1
					PENPKQAYQKRMTR/GLF	
					PENPKQAYKKRMTR/GLF	
					PENPKQAYHKRMTR/GLF	
					PENPKQAHQKRMTR/GLF	
					PENPRQAYRKRMTR/GLF	
					PENPKQACQKRMTR/GLF	
H7N1	LP	UAE	2004	A/houbara bustard/UAE/2004	PELPKRR/GLF	

Figure S3 Sequence at HA cleavage site determines pathogenicity.

https://dx.doi.org/10.21037/jtd-21-226